Journal of Biomedical Optics

SPIEDigitalLibrary.org/jbo

Economic and simple system to combine single-spot photolysis and whole-field fluorescence imaging

Nadia Jaafari
Mark Henson
Jeremy Graham
Marco Canepari

SPIE

Economic and simple system to combine single-spot photolysis and whole-field fluorescence imaging

Nadia Jaafari,[a,b,c] Mark Henson,[d] Jeremy Graham,[d] and Marco Canepari[a,b,c]
[a]Inserm U836, Team 3, Grenoble Cedex 09, France
[b]Université Joseph Fourier, Grenoble Institut des Neurosciences and Laboratoire Interdisciplinare de Physique (CNRS UMR 5588), France
[c]Ion Channel Science and Therapeutics, Laboratories of Excellence
[d]CAIRN Research Ltd., Faversham, UK

Abstract. In recent years, the use of light emitting diodes (LEDs) has become commonplace in fluorescence microscopy. LEDs are economical and easy to couple to commercial microscopes, and they provide powerful and stable light that can be triggered by transistor-transistor logic pulses in the range of tens of microseconds or shorter. LEDs are usually installed on the epifluorescence port of the microscope to obtain whole-field illumination, which is ideal for fluorescence imaging. In contrast, photolysis or channelrhodopsin stimulation often requires localized illumination, typically achieved using lasers. Here we show that insertion of a long-pass (>411 nm) filter with an appropriately sized pinhole in the epifluorescence pathway, combined with dual UV/visible illumination, can produce efficient whole-field visible illumination and spot UV illumination of 15 to 20 μm. We tested our system by performing calcium imaging experiments combined with L-glutamate or *N*-methyl-D-aspartic acid (NMDA) photorelease in hippocampal neurons from brain slices or dissociated cultures, demonstrating the ability to obtain local activation of NMDA receptors exclusively in the illuminated spot. The very inexpensive and simple system that we report here will allow many laboratories with limited budgets to run similar experiments in a variety of physiological applications. © *2013 Society of Photo-Optical Instrumentation Engineers (SPIE)* [DOI: 10.1117/1.JBO.18.6.060505]

Keywords: photolysis; calcium imaging; light emitting diode illumination; epifluorescence microscope.

Paper 130303LR received May 2, 2013; revised manuscript received May 16, 2013; accepted for publication May 16, 2013; published online Jun. 13, 2013.

1 Introduction

For functional imaging applications, solid-state lasers and light emitting diodes (LEDs) are progressively replacing the arc lamps or lamp-based illumination systems that were routinely used for more than three decades.[1] Modern solid-state lasers provide high-power, stable, and monochromatic illumination, but despite typically delivering fewer photons to the sample, several advantages make LEDs preferable in many situations. First, LEDs are cheaper, more compact, and easier to control and can be powered by a constant current source and triggered by transistor-transistor logic pulses with microsecond precision. Second, LEDs produce incoherent light over a wide range of angles, which can be easily collimated and mounted onto the standard epifluorescence port of commercial microscopes to obtain nearly uniform illumination of the whole visual field, which is ideal for fluorescence imaging using a camera. Third, LEDs are safer and do not produce the laser speckle associated with coherent light sources, while they can still be cascaded to obtain multicolor illumination. The light of LEDs, although less powerful than that of lasers, is bright enough not only for fluorescence excitation but also for photostimulation, for instance, for activation of channelrhodopsin (ChR)[2] or for molecular photorelease from caged compounds.[3] However, some applications require local photostimulation and, therefore, illumination from relatively small spots. Diffraction limited spots of <1 μm can only be generated using a laser.[4] Nevertheless, lasers are more difficult to work with, and because they produce a tight collimated beam, require more stringent safety procedures, which are not always convenient when working with physiological preparations. Thus, it is extremely useful to explore to what extent local photostimulation can be achieved, in a simpler and cheaper way using LED illumination. To investigate this possibility, we used the flexibility of the Olympus BX microscope, which has an adjustable field stop designed to reduce the field of fluorescence illumination. We replaced this field stop with a device where we alternatively mounted pinholes of different sizes, drilled through 411-nm long-pass (LP) filters. In this way, we could combine local UV illumination and whole-field visible illumination. As the light intensity decreased with the diameter of the UV spot, we found that the intensity is still >10% for a spot of 15 to 20 μm and sufficient to obtain significant photolysis using short pulses from commonly used 4-methoxy-7-nitroindolinyl (MNI) caged compounds.

2 Materials and Methods

Experiments were performed using an Olympus BX51 microscope equipped with a 60 × /1.0 NA Nikon objective. A dual-port coupler for LEDs, equipped with a 409-nm dichroic mirror (FF409, Semrock, Rochester, New York), was mounted on the epifluorescence port of the microscope. A 365-nm LED controlled by an OptoFlash (CAIRN Research Ltd., Faversham, UK) and 470-nm LED controlled by an OptoLED (also from Cairn) were mounted on the two ports of the coupler and used for uncaging and fluorescence excitation, respectively.

Address all correspondence to: Marco Canepari, INSERM U836–Grenoble Institute of Neuroscience, Bâtiment Edmond Safra, Chemin Fortune Ferrini, Site santé de la Tronche–BP 170, 38042 Grenoble cedex 9, France. Tel: +33 4 565200565; E-mail: marco.canepari@ujf-grenoble.fr

0091-3286/2013/$25.00 © 2013 SPIE

A silica condenser lens was used with the ultraviolet LED, which allowed full-field illumination if required. Alternative optics to concentrate light over a smaller area may allow throughput improvements in future, but the purpose of this paper was to investigate the diffractive losses associated with masking a full-field beam. To manufacture LP pinholes, holes of 100, 150, 200, and 300 μm were drilled by Small Hole Drilling s.r.o. (Náměšť nad Oslavou, Czech Republic) on 411-nm LP Wratten gelatin filters (411 WY 75, Comar, Cambridge, UK) and mounted on a black plastic ring. The ring, shown in the bottom picture of Fig. 1(a) on the right, was inserted in a custom-made slider [bottom picture of Fig. 1(a) left] to replace the field stop of the Olympus BX51 microscope, as illustrated in the top picture of Fig. 1(a). The position of the pinhole, relative to the specimen, could be adjusted with two screws, in our case in the middle of the field of view of the CCD camera used for imaging. This device is now commercially available from Cairn. The LED light downstream of the LP pinhole was directed to the objective [Fig. 2(b)] using a 506-nm dichroic mirror (FF506, Semrock), and fluorescence emission was filtered at 510 ± 42 nm, demagnified by 0.5×, and acquired using a NeuroCCD-SM camera (RedShirtImaging LLC, Decatur, Georgia) at 1000 frames/s. Calcium fluorescence signals were expressed as fractional changes of fluorescence ($\Delta F/F_0$). Hippocampal slices (250 μm thick) were prepared from a 32-postnatal-days old C57Bl6 mouse using a VF-200 compresstome (Precisionary Instruments, Greenville, North Carolina). Experiments were approved by the Isere prefecture (Authorization n. 38 12 01) and the specific protocol (n. 197) by the ethics committee of the Grenoble Institute of Neuroscience. Hippocampal cell cultures were prepared from embryonic day 18 (E18) rat embryos by the laboratory of Yves Goldberg as described in Belly et al.[5] and used after two weeks. The extracellular solution used in our recordings contained (mM): 125 NaCl, 26 $NaHCO_3$, 20 glucose, 3 KCl, 1 NaH_2PO_4, 2 $CaCl_2$, and 0.001 tetrodotoxin bubbled with 95% O_2 and 5% CO_2. The intracellular solution contained (mM): 125 $KMeSO_4$, 5 KCl, 8 $MgSO_4$, 5 Na_2-ATP, 0.3 Tris-GTP, 12 tris-phosphocreatine, and 20 HEPES, adjusted to pH 7.35 with KOH. Calcium indicators, either Oregon Green 5N (OG5N) or Oregon Green BAPTA-1 (OGB1) were purchased from Invitrogen (Carlsbad, California) and added at a concentration of 500 μM to the internal solution. Patch-clamp recordings were made using a multiclamp amplifier 700 A (Molecular Devices, Sunnyvale, California). Photorelease of L-glutamate or *N*-methyl-D-aspartic acid (NMDA) was produced from the caged compounds MNI-glutamate[6] and MNI-NMDA,[7] purchased from Tocris (Bristol, UK). Caged compounds were dissolved at 1 mM concentration in extracellular solution and applied locally near the cell with a large pipette to obtain a uniform concentration in the area of photolysis while avoiding light absorption in the pathway from the objective to the cell.

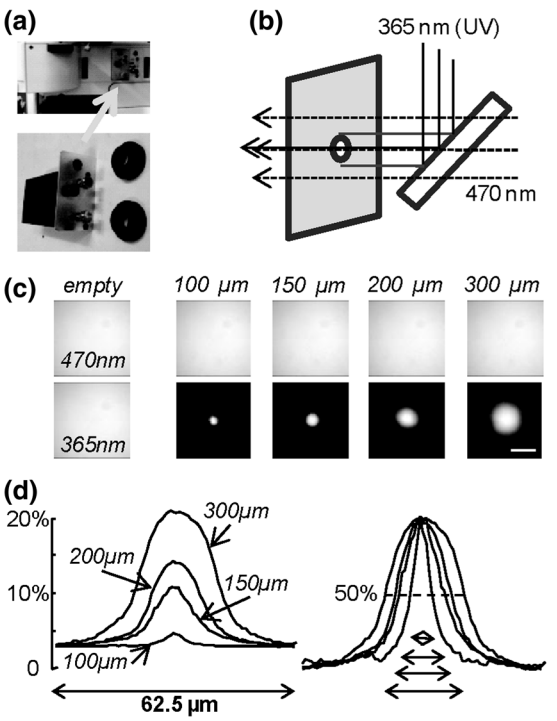

Fig. 1 LED illumination with LP pinholes. (a) Picture of a device designed for Olympus BX microscopes to insert and position LP pinholes in the epifluorescence pathway (left); gelatin filters where the pinholes were drilled glued on plastic rings and placed in the device (right). (b) Scheme of the 365/470 nm illumination; LP pinholes produce whole-field visible illumination and spot UV illumination. (c) Illumination patterns at 470 and 365 nm with a 60× objective (top); patterns correspond to illumination without pinholes and with 100, 150, 200, and 300 μm pinholes; scale bar 20 μm. (d) Illumination profiles of a pixel line in the middle row of the image; left: profiles normalized to image without pinhole; right: profiles normalized to their maxima; spot diameters with more than 50% of the light intensity (double arrows) were 6, 11.5, 14.5, and 20.5 μm.

3 Results

The goals of this work were (1) to quantify the intensity and spatial distribution of UV light through LP pinholes and (2) to test whether UV light through LP pinholes could produce efficient and localized photolysis from commercial caged compounds in simple proof-of-principle uncaging/Ca^{2+} experiments in cellular preparations. Figure 1(c) shows images from a fluorescent slide, illuminated either at 470 or at 365 nm, without any pinhole or with pinholes of diameters 100, 150, 200, and 300 μm. These images illustrate that the UV illumination is concentrated in spots of ~10, 15, 20, and 30 μm, respectively. To quantify the spatial profile of the UV illumination with the pinholes, we plotted the light intensity in the central row, normalized to the maximal intensity without the pinhole [Fig. 1(d) left] and to the maximal intensity with the pinholes [Fig. 1(d) right]. The first plot shows that the light intensity with the pinholes, reduced by diffraction, is, respectively, 5, 10, 15, and 21% of the maximal intensity without the pinhole, including a background of 3% of bleedthrough passing through the gelatin filter. The second plot shows that for the four pinholes, the diameters within which the light intensity is >50% of its maximum are 6, 11.5, 14.5, and 20.5 μm, respectively. The power of our 365-nm LED at the back-aperture of the objective is >50 mW. This power produces very efficient photolysis from MNI-caged compounds with light exposures >100 μs. Thus, we expected to obtain efficient photolysis with light pulses >1 ms through the 150 to 200 μm pinholes. To test this hypothesis in a biological application, we filled a CA1 hippocampal pyramidal neuron from a brain slice with the low-affinity indicator OG5N [$K_d = 35$ μM (Ref. 8)] and measured the $\Delta F/F_0$ Ca^{2+} signal via NMDA receptors (NMDARs) generated by L-glutamate uncaging with pulses of 1 to 4 ms using the 150-μm LP pinhole [Fig. 2(a)]. To mimic a physiological scenario, we uncaged

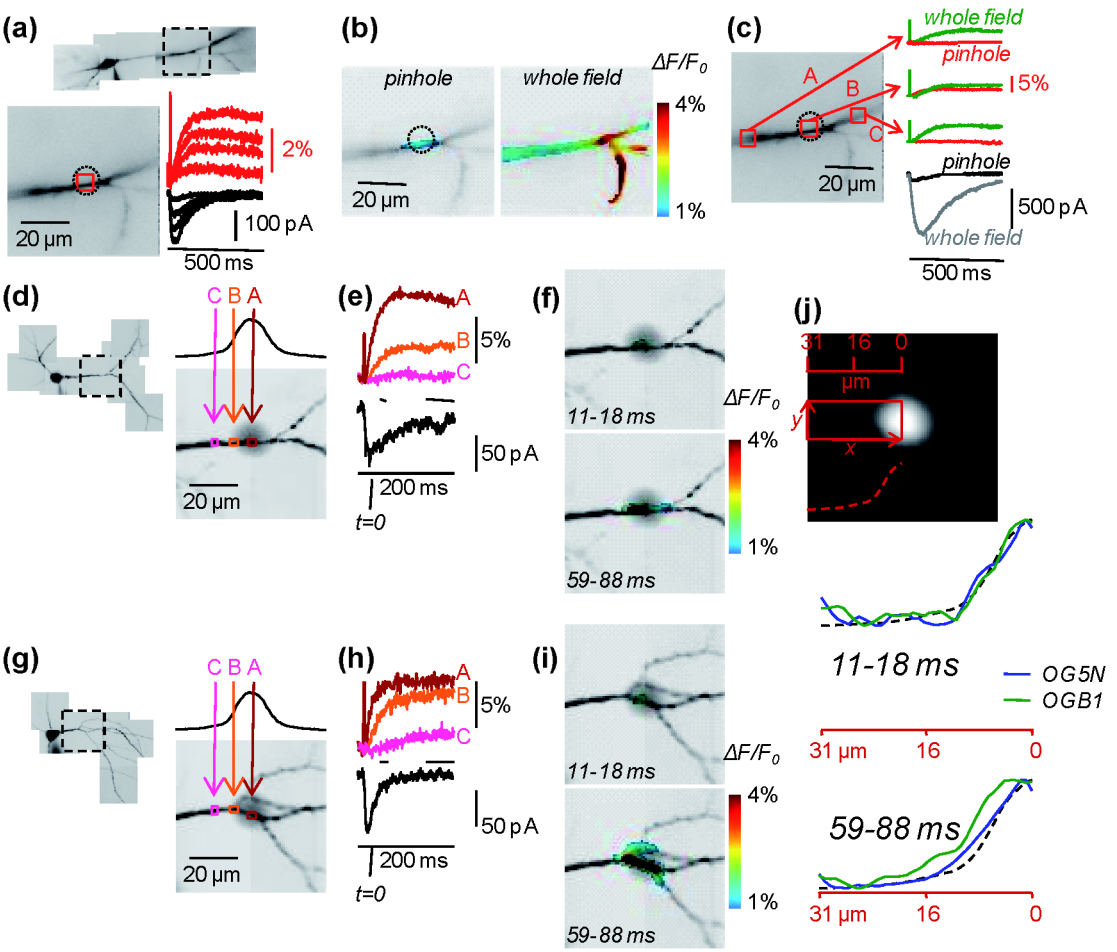

Fig. 2 Simultaneous photolysis and Ca^{2+} imaging. (a) Reconstruction of a hippocampal neuron filled with 500 μM OG5N; in the recording position image below the UV spot (150 μm pinhole) represented by a dotted circle; red and black traces are respectively the $\Delta F/F_0$ Ca^{2+} signals in the red square and the somatic currents associated with UV flashes of 1, 2, 3, and 4 ms uncaging glutamate. (b) Spatial distributions of $\Delta F/F_0$ superimposed to the image represented in a color scale during the period of 150 to 200 ms after a 3 ms pinhole UV flash (left) and after a 0.2 ms whole-field UV flash (right). (c) $\Delta F/F_0$ signals after the pinhole UV flash (red traces) and after the whole-field UV flash (green traces) in the three regions A to C indicated on the left image; correspondent somatic currents are indicated below. (d) Reconstruction of a cultured hippocampal neuron filled with 500 μM OG5N; in the recording position image on the right, the position of the UV spot (200 μm pinhole) is represented by a gray shadow; the colored frames indicate three regions of interest (A, B, and C) in the middle of the spot, in the periphery, and outside the spot. (e) $\Delta F/F_0$ associated with a UV flash (occurring at $t = 0$) uncaging NMDA from the regions A to C in (d); somatic recording of the NMDA current is shown below (black trace); duration of UV flash is 2 ms. (f) Spatial distribution of $\Delta F/F_0$ superimposed to the image represented in a color scale during the periods of 11 to 18 and 59 to 88 ms after the UV flash ($t = 0$). (g) through (i) Same as A to C in another cultured hippocampal neuron filled with OGB1. (j) Another picture of the 200 μm pinhole with a rectangle of 40 × 16 pixels ($x \times y$ axes); the dotted line represents the profile of UV light intensity averaged over the 16 pixels on y axis as a function of the distance of the pinhole center; below, superimposed to the UV light intensity profile, the profiles of normalized $\Delta F/F_0$ during the periods of 11 to 18 and 59 to 88 ms after the UV flash ($t = 0$) as a function of the distance of the pinhole center.

L-glutamate onto a spot in the main apical dendrite located ~100 μm from the soma where Shaffer collateral synapses are expected to form. We then compared the spatial distribution of the $\Delta F/F_0$ signal generated by a 3-ms UV pulse through the 150-μm LP pinhole with that generated by a 200-μs UV pulse without pinhole [Fig. 2(b)]. As shown in Fig. 2(c), the amplitude of the $\Delta F/F_0$ signal in the two cases is similar in the photolysis spot (dotted circle), but Ca^{2+} elevation outside the spot is observed only without the LP pinhole, in agreement with the larger somatic current recorded with the patch-clamp electrode [Fig. (2c) bottom-left]. A Ca^{2+} elevation outside the spot was, however, still observed with the LP pinhole for pulses >5 ms (data not shown). This phenomenon could be due to the leak of UV light through the gelatin filter and the L-glutamate diffusion after photorelease. Thus, to quantitatively test photolysis localization with short pulses, we performed experiments of NMDA photorelease in dissociated cultures. For our purpose, experiments in cultures have two advantages. First, the caged compound applied extracellularly equilibrates by diffusing in free space and it is uniform over the area of UV illumination. Second, the released NMDA also equilibrates by diffusion in the free space, interacting exclusively with NMDARs and not to other receptors or to glutamate transporters. The hippocampal cell in Fig. 2(d) was filled with 500 μM of OG5N. In the image of the recording position on the left, we added a dark shadow to indicate the region of the UV spot and selected three regions of interest (A, B, and C) in the middle, in the periphery, and outside the spot. Figure 2(e) shows the NMDA current and the associated $\Delta F/F_0$ signals in regions A to C following a 2-ms UV pulse through the 200 μm pinhole. The spatial profiles of $\Delta F/F_0$, averaged over two time windows (11 to 18 and 59 to 88 ms) are illustrated in Fig. 2(f) using a color scale. The spatial

profile of activated NMDARs does not necessarily coincide with that of photolysis because NMDARs can also be activated by lateral diffusion of NMDA from the uncaging site. In addition, the spatial profile of Ca^{2+} fluorescence evolves following diffusion of the indicator bound to Ca^{2+}. This component, however, depends on the affinity of the indicator since Ca^{2+} unbinding from high-affinity indicators is slower. Thus, to appreciate this effect, we repeated the same experiment in another cell [Fig. 2(g)] filled with 500 μM of the high-affinity indicator OGB1 [$K_d = 200$ nM (Ref. 9)]. As shown in the traces of Fig. 2(h) and from the averaged $\Delta F/F_0$ profiles in Fig. 2(i), the Ca^{2+} bound to OGB1 is initially observed exclusively in the spot and later diffuses outside the spot, an effect less evident with OG5N. We further analyze the UV illumination profile and Ca^{2+} fluorescence averaged over the two time windows of Fig. 2(f) and 2(i) in the rectangular region depicted in Fig. 2(j) (left). In particular, we averaged light intensities over the y axis and plotted the results over the x axis as a function of the distance from the point of maximal UV illumination. This analysis allows a comparison of distributions of UV light intensity and of $\Delta F/F_0$ signals in the two time windows. The x-profiles of $\Delta F/F_0$ signals at 11 to 18 ms after UV exposure remarkably match the profile of UV illumination. In contrast, $\Delta F/F_0$ signals are clearly present outside the UV spot at 59 to 88 ms after UV exposure. Because the non-co-localized signal is much larger with OGB1, we conclude that this effect is due to the diffusion of the bound indicator and not due to the photoreleased NMDA. The same analysis also indicates that the contribution of NMDA photorelease by the UV leak through the gelatin filter is negligible. We can therefore conclude that the profile of NMDARs activation matches that of the UV spot that we created with the pinhole.

4 Discussion

Combining photostimulation with Ca^{2+} imaging[8] or voltage imaging[10] is important to address a variety of physiological questions. Some experiments can be performed by illumination of the whole field of view using either a flash-lamp[11] or an LED. In contrast, local photostimulation is typically achieved using lasers. Thus, one-photon[4] or two-photon[12] laser photostimulation permits illumination of spots <1 μm, i.e., an area close to that of a dendritic spine. The implementation of laser photostimulation, however, can be expensive and difficult to combine with other illumination systems used for fluorescence excitation. For this reason, we explored to what extent useful local photostimulation could be achieved using a simple and economic multicolour LED system that is simultaneously used for fluorescence excitation. We implemented this solution by inserting an LP filter with a pinhole in the illumination pathway. The localization of small spots is less precise than would be predicted by the magnification of the objective lens and epicondenser optics and is instead limited by diffraction, which also reduced the light intensity in the illuminated area. The practical question we addressed was, therefore, to find out the smallest spot size that could allow efficient and local photolysis. We have shown here that this could be achieved with MNI-caged compounds in spots of 15 to 20 μm using illumination pulses of 1 to 4 ms. The size of this spot is sufficiently small for many photolysis applications, including extrasynaptic activation of receptors or local activation of intracellular pathways. The principle of drilling a pinhole in an LP filter can be extended to longer wavelengths permitting local ChR stimulation and imaging with a combination of blue and green or red light illumination. In conclusion, this solution is now commercially available and we foresee that it will be adopted by several laboratories.

Acknowledgments

We thank Dr. Yves Goldberg and Dr. José Martínez Hernández for providing the hippocampal cultures used in our experiments, Philippe Moreau for technical help, and Jean-Claude Vial for useful discussions. All experiments were performed at the Laboratoire Interdisciplinaire de Physique of the Joseph Fourier University. This work was supported by the Agence Nationale de la Recherche (Grant Voltimagmicro, program Emergence-10 and Labex Ion Channels Science and Therapeutics).

References

1. L. A. Thomson and G. J. Hageage, "Evaluation of excitation light sources for incident immunofluorescence microscopy," *Appl. Microbiol.* **30**(4), 616–624 (1975).
2. F. Zhang et al., "Channelrhodopsin-2 and optical control of excitable cells," *Nat. Methods* **3**(10), 785–792 (2006).
3. J. A. McCray and D. R. Trentham, "Properties and uses of photoreactive caged compounds," *Annu. Rev. Biophys. Biophys. Chem.* **18**, 239–270 (1989).
4. F. F. Trigo, J. E. Corrie, and D. Ogden, "Laser photolysis of caged compounds at 405 nm: photochemical advantages, localisation, phototoxicity and methods for calibration," *J. Neurosci. Methods* **180**(1), 9–21 (2009).
5. A. Belly et al., "CHMP2B mutants linked to frontotemporal dementia impair maturation of dendritic spines," *J. Cell Sci.* **123**(17), 2943–2954 (2010).
6. M. Canepari et al., "Photochemical and pharmacological evaluation of 7-nitroindolinyl-and 4-methoxy-7-nitroindolinyl-amino acids as novel, fast caged neurotransmitters," *J. Neurosci. Methods* **112**(1), 29–42 (2001).
7. F. Palma-Cerda et al., "New caged neurotransmitter analogs selective for glutamate receptor sub-types based on methoxynitroindoline and nitrophenylethoxycarbonyl caging groups," *Neuropharmacology* **63**(4), 624–634 (2012).
8. M. Canepari and D. Ogden Kinetic, "Pharmacological and activity-dependent separation of two Ca^{2+} signalling pathways mediated by type 1 metabotropic glutamate receptors in rat Purkinje neurons," *J. Physiol.* **573**(1), 65–82 (2006).
9. M. Maravall et al., "Estimating intracellular calcium concentrations and buffering without wavelength ratioing," *Biophys. J.* **78**(5), 2655–2667 (2000).
10. K. E. Vogt et al., "Combining membrane potential imaging with L-glutamate or GABA photorelease," *PLoS One* **6**(10), e24911 (2011).
11. G. Rapp, "Flash lamp-based irradiation of caged compounds," *Methods Enzymol.* **291**, 202–222 (1998).
12. D. L. Pettit et al., "Chemical two-photon uncaging: a novel approach to mapping glutamate receptors," *Neuron* **19**(3), 465–471 (1997).